Available online at www.sciencedirect.com

SciVerse ScienceDirect

Ceramics International 39 (2013) 1729–1739

CERAMICS INTERNATIONAL

www.elsevier.com/locate/ceramint

The phase formation and stability of tetragonal ZrO_2 prepared in a silica bath

Hung-Jui Huang, Moo-Chin Wang*

Department of Fragrance and Cosmetic Science, Kaohsiung Medical University, 100 Shih-Chuan 1st Road, Kaohsiung 80782, Taiwan

Received 28 May 2012; received in revised form 8 August 2012; accepted 8 August 2012
Available online 23 August 2012

Abstract

Tetragonal zirconia (ZrO_2) precursor powders were obtained in a silica bath using zirconium (IV) nitrate and tetraethyl orthosilicate (TEOS) as starting materials in an ethanol–water solution using co-precipitation process mixing at 348 K and pH = 7 for 10 min. The phase formation and stability of ZrO_2 freeze dried precursor powders prepared in a silica bath were investigated using differential scanning calorimetry/thermogravimetry (DSC/TG), X-ray diffraction (XRD), transmission electron microscopy (TEM), selected area electron diffraction (SAED) and an energy dispersive spectrometer (EDS). DSC results revealed tetragonal ZrO_2 (t-ZrO_2) formation at 1165 K. After the zirconia freeze dried precursor powders were calcined between 1173 K and 1473 K for 2 h, XRD patterns showed the calcination powders all to be a single tetragonal phase. The crystallite size of the tetragonal zirconia was only 3.3 nm when the freeze-dried precursor powders were calcined at 1173 K for 10 min. In addition, the crystallite size of t-ZrO_2 increased but was still smaller than 20 nm when the freeze dried precursor powders were calcined at 1473 K for 120 min. The TEM observed results were also confirmed with XRD analysis.

Key words: Tetragonal zirconia; Phase stability; Co-precipitation process; Silica bath

1. Introduction

Zirconia (ZrO_2) is derived from zircon and baddeleyite in nature, and it has three polymorph forms depending on various temperatures. Monoclinic ZrO_2 (m-ZrO_2) exists at temperatures lower than 1443 K. Tetragonal ZrO_2 (t-ZrO_2) exists between 1443 and 2643 K. When temperatures are higher than 2643 K, the phase transition from t-ZrO_2 to cubic ZrO_2 (c-ZrO_2) occurs [1]. Zirconias are important ceramic materials for a broad range of applications. The traditional applications of ZrO_2 are use as refractory ceramics and abrasion-resistant materials. In addition, due to the fact that ZrO_2 possesses the properties of high strength and toughness, good wear resistance, hardness, and thermal shock resistance, it has many engineering applications, such as use in automobile engine parts, exhaust parts, brake parts and cutting tools [2]. Moreover, also ZrO_2 is an appropriate material for thermal barrier coatings on metal components because it has a relatively high thermal expansion coefficient (compared to many other ceramics) and low thermal conductivity [3].

However, pure ZrO_2 ceramics can displacive the t-ZrO_2 to m-ZrO_2 phase transformation occurs at about 1443 K on cooling in pure ZrO_2, which is accompanied by a volume expansion and a shear strain of ~4% and ~0.16, respectively. Unaccommodated, the phenomenon of volume change and it results on shape in the transformation process can result in fractures and, therefore, structural unreliability of fabricated components [4]. Thus, Garvie et al. [5] have pointed that out alloy systems based on zirconia can exhibit improved strength and a high degree of toughness. Furthermore, an effort to understand the meanings and applications of transformation in order to enhance the mechanical properties has also been reported by many previous researchers [6–8], and it has been suggested that the transformation from tetragonal to monoclinic ZrO_2 might be controlled and thus enhance properties related to the development of improved

*Corresponding author. Tel.: +886 7 3121101x2366; fax: +886 7 3210683.
E-mail address: mcwang@kmu.edu.tw (M.-C. Wang).

0272-8842/$ - see front matter © 2012 Elsevier Ltd and Techna Group S.r.l. All rights reserved.
http://dx.doi.org/10.1016/j.ceramint.2012.08.019

engineering ceramics. The investigation of toughening in ceramic systems has also been reported by Heuer [2] and Evans [9].

To avoid the phase transformation that occurs when shifting from higher temperatures as it cools to room temperature, the addition of 8 mol% Y_2O_3 to pure ZrO_2, forming a yttria stabilized ZrO_2 (8YSZ) ceramic with a single cubic phase for high temperature applications, has been demonstrated by Pascual and Duran [10]. When ZrO_2 contains 3∼6 mol% yttria, this can result in the t-phase becoming the primary phase. The definition of partially stabilized ZrO_2 (PSZ) is that both phases of t-ZrO_2 and m-ZrO_2 coexist in a matrix. On the other hand, when the phase content is almost tetragonal, this is defined as tetragonal ZrO_2 polycrystals (TZP).

For the purpose of more applications, the tetragonal phase of zirconia stabilized at room temperature is very important. With the exception of decreases in crystallite size [5], other various processes have also been used to obtain t-ZrO_2. Their routes to attain the stabilization of tetragonal ZrO_2 have included the addition of yttria (Y_2O_3) and use of a coprecipitation process [11–13], neodymia-doped ZrO_2 using a sol–gel method [14], ceria-stabilized ZrO_2 using spray drying [15], the preparation of tantalum ion-doped t-ZrO_2 using a polymer matrix-based precursor solution method [16], low temperature metastabilization of tetragonal vanadium-ZrO_2 solid solution using a gelling mixtures process [17], and t-ZrO_2 doped with nickel oxide using a chemical precipitation process [18]. However, obtaining t-ZrO_2 prepared in a silica bath has not been discussed in detail.

Other work has examined the effect of coatings on phase stability in silica-encapsulated metal nanoshells [19] and zirconia-coated silica particles [20] with results indicating that surface coatings can inhibit melting in nanoshells and that coating materials do not crystallize in the same manner as bulk species. Silicate glass-coated zirconia particles [21,22], and silica-coated silicon particles [23] have also been studied, and the findings have shown that crystallites in the size range of hundreds of nanometers to micrometers can be stabilized in certain phases by altering their surfaces with a coating.

In the present contribution, the effect of particle interfacial chemistry on phase stability is explored in zirconia nanoparticles on the order of 20 nm in diameter. The tetragonal zirconia nanoparticles examined have no added dopants and are stabilized only by finite size effects. The tetragonal zirconia particle is isolated domains, and the tetragonal particles are single crystallites prepared under co-precipitation conditions. The zirconia is then coated with a silica surface layer using solution phase hydrolysis chemistry. The products are also isolated particles treated as silica nucleates only on the surface of the zirconia cores, rather than as separate colloidal entities in solution.

In the present study, zirconia (IV) nitrate ($Zr(NO_3)_4 \cdot xH_2O$) and tetraethyl orthosilicate (TEOS) are used as the starting materials for synthesis of the tetragonal ZrO_2 nanocrystallites by a coprecipitation process. The major purpose of the present study is to inspect the phase transformation and stability of the tetragonal ZrO_2 prepared in a silica bath using thermogravimetric and differential scanning calorimetry (TG/DSC), X-ray diffraction (XRD), transmission electron microscopy (TEM), selected area electron diffraction (SAED), and an energy dispersive spectrometer (EDS).

This work investigates: (i) the thermal behavior of the ZrO_2 freeze dried precursor powders, (ii) the phase transformation of the ZrO_2 freeze dried precursor powders prepared in a silica bath, (iii) the phase stability of tetragonal ZrO_2, and (iv) the TEM microstructure of ZrO_2 freeze dried precursor powders is observed after calcination at various temperatures and times.

2. Experimental procedures

2.1. Sample preparation

Zirconium (IV) nitrate ($Zr(NO_3)_4 \cdot xH_2O$, purity∼99.5%, supplied by Acros Organics, Belgium) and tetraethyl orthosilicate (TEOS, $(C_2H_5O)_4Si$, purity∼99.0%, supplied by Merck, Germany) were used as the starting materials for the coprecipitation process. Zirconium nitrate was dissolved in a solution of deionized water mixed ethanol with a volume ratio of 1:5. A molar ratio of Zr/Si equal to 1 in solution was prepared, and the mixed solution was stirred using a magnetic stirrer and heated to 348 K. NH_4OH (Nihon Shiyaku Reagent, Japan) as a precipitator was slowly added to the solution until it reached a pH of 7. After precipitation, the precipitates were repeatedly rinsed with 2 l of deionized water, and then the precursor powders were freeze-dried at 223 K in a vacuum.

2.2. Sample characterization

A DSC/TG (SDT Q600, TA, USA) was conducted in the temperature range of 323–1473 K in static air. Approximately 8 mg of freeze-dried precursor powders were heated at various rates. Al_2O_3 powders were used as a reference material. The calcination temperature was determined from the DSC results.

The crystalline phase was identified by XRD (Rigaku, Ultima IV, Japan) with Cu Kα radiation and a Ni filter, operating at 40 KV, 30 mA and scanning at a rate of $1^\circ\,min^{-1}$. The crystallite size of the t-ZrO_2 was calculated by using Scherrer's equation [24]:

$$d = \frac{0.9\lambda}{\beta \cos\theta}, \tag{1}$$

where λ is a wavelength of the X-ray (1.542 Å); β and θ represent the measured full-width at half-maximum of the peak and a diffraction angle, respectively.

The morphology of the zirconia freeze dried precursor powders calcinated at various temperatures for 120 min were examined using TEM (JEM2100F, JEOL, Japan) operating

at 200 KV. SAED and EDS (INCA TEM250, Oxford, UK) examinations were also conducted on the powders.

3. Results

3.1. Thermal behavior of ZrO_2 freeze-dried precursor powders

Fig. 1 shows the DTA/TG curves for the ZrO_2 freeze-dried precursor powders heated from 300 to 1473 K in static air at a heating rate of 5 K min^{-1}. The TG curve can be divided to four major weight loss stages: (i) 298–307 K, (ii) 307–428 K, (iii) 428–552 K and (iv) 552–1289 K.

In the first stage, the weight loss of about 3.6% was determined to be due to the dehydration and evaporation of water on the surface of the precursor powders [13]. In the second stage, about 12.6% weight loss occurred, which was caused by the following reaction [13]:

$$[Zr_4(OH)_8][OH]_8 \rightarrow [Zr_4(OH)_4O_4][OH]_4 + 4H_2O. \quad (2)$$

This is because the square-arranged Zr atoms were linked by four OH groups and four O atoms in the $[Zr_4(OH)_4O_4]^{4+}$ cation.

In the third stage, 428–522 K, a weight loss of about 4.7% is attributed to the reaction from $[Zr_4(OH)_4O_4][OH]_4$ losing $2H_2O$. This result can be expressed as following reaction:

$$[Zr_4(OH)_4O_4][OH]_4 \rightarrow [Zr_4(OH)_2O_6][OH]_2 + 2H_2O. \quad (3)$$

In the final stage, 522–1289 K, a weight loss of about 3.4% resulted. This was because of the reaction from $[Zr_4(OH)_2O_6][OH]_2$ losing $2H_2O$ leading to the following ZrO_2 formation:

$$[Zr_4(OH)_2O_6][OH]_2 \rightarrow 4ZrO_2 + 2H_2O. \quad (4)$$

Above 1289 K, there was no further weight loss until a temperature of 1473 K was reached.

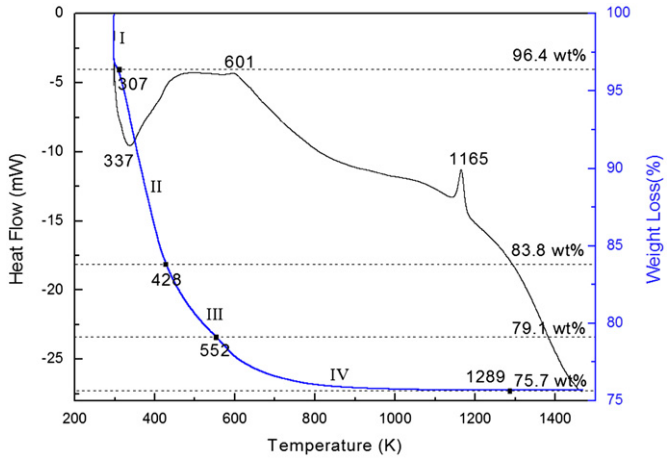

Fig. 1. The DSC/TG curves of the tetragonal zirconia freeze dried precursor powders prepared in silica bath at a heating rate of 5 K min^{-1} in static air from 300 to 1473 K.

In addition, the DSC curve shows two exothermic peaks at 601 K and 1165 K. The first exothermic peak at 601 K was attributed to a dehydration reaction leading to the atomic prearrangement of the tetragonal structure, which caused the freeze-dried precursor powders to approach a more stable state [25], accompanied by a small amount of decomposition of NH_2^- into N_2 and H_2 [26]. The second exothermic peak at 1165 K was related to the crystalline of the tetragonal zirconia formation from the amorphous freeze-dried precursor powders.

3.2. The phase transformation of the ZrO_2 freeze-dried precursor powders after calcination

Fig. 2 shows the XRD patterns of the ZrO_2 freeze-dried precursor powders prepared in a silica bath calcined at various temperatures for 10 min. The XRD pattern of the ZrO_2 as freeze dried precursor powders is shown in Fig. 2(a), which reveals that the precursor powders maintained their amorphous state. Fig. 2(b) shows the XRD pattern of the ZrO_2 freeze dried precursor powders calcined at 673 K for 10 min, which reveals that the precursor powders still maintained their amorphous state. This result is due to the fact that the ZrO_2 freeze dried precursor powders calcined at 673 K do not obtain enough energy for amorphous state atoms to rearrange at the lattice site, leading to ZrO_2 crystallization. Fig. 2(c) illustrates the XRD pattern of the ZrO_2 freeze dried precursor powders calcined at 1173 K for 10 min. Only a single phase of tetragonal zirconia (t-ZrO_2) can be seen.

Moreover, a broadening and weak intensity of the t-ZrO_2 reflections is also seen in Fig. 2, and this is attributed to poor crystallinity and/or to the crystallite size of the t-ZrO_2 powders being in the submicron to

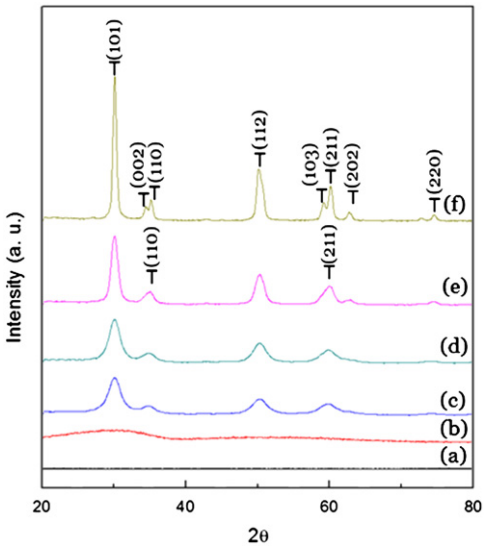

Fig. 2. XRD patterns of the tetragonal zirconia freeze dried precursor powders are calcined at various temperatures for 10 min: (a) as freeze-dried state, (b) 673 K, (c) 1173 K, (d) 1273 K, (e) 1373 K and (f) 1473 K. (T: tetragonal zirconia).

nanometers scale [27,28]. On the other hand, the DTA curve (Fig. 1) shows that the crystallization of the ZrO_2 freeze dried precursor powders occurred at 1165 K. The results shown in Fig. 2(c) also correspond to the results of the DTA curve. The XRD pattern for the ZrO_2 freeze dried precursor powders calcined at 1273 K for 10 min is shown in Fig. 2(d), which reveals that although the phase still maintained the t-ZrO_2, the intensity of the reflection peaks are still weak and broadened. Fig. 2(e) shows the XRD pattern of the ZrO_2 freeze-dried precursor powders calcined at 1373 K for 10 min, and it can be seen that the intensity of the reflections peaks exhibits greater increases than was seen in the calcination at 1173 and 1273 K (Fig. (c) and (d)). This phenomenon is attributed to the fact that the crystallinity of the t-ZrO_2 improved with rises in the calcination at 1373 K. The XRD pattern of the ZrO_2 freeze dried precursor powders calcined at 1473 K for 10 min is shown in Fig. 2(f). It reveals a very sharp and narrow peak of (101) reflection. In addition, the t-ZrO_2 reflections of (002) and (110) at about 35.2°, (103) and (211) at about 60.2° are gradually split with rises in calcination temperature. This result is because the phase conversion reaction increased with rises in the calcination temperature and thus enhanced the ability of the ZrO_2 atoms to obtain enough energy for rearrangement and crystallization, leading to the formation of more t-ZrO_2, which promoted a stable t-ZrO_2lattice structure.

In Fig. 1, the exothermic temperature of t-ZrO_2 crystallization occurred at 1165 K. In order to understand the phase transition behavior of ZrO_2 freeze-dried precursor powders after calcination at fixed temperature for various times, the ZrO_2 freeze-dried precursor powders are calcined at temperatures slightly higher than 1165 K for various periods of time. Fig. 3(a) shows the XRD pattern of the ZrO_2 freeze-dried precursor powders calcined at 1173 K for 10 min, and it can be seen that the (101), (110), (112) and (211) reflections of t-ZrO_2 appear to have poor crystallinity and to be broadened. The XRD pattern of the ZrO_2 freeze dried precursor powders calcined at 1173 K for 20 min are shown in Fig. 3(b). It can be seen that only the t-ZrO_2 appears, but the intensity of the peaks still is weakened and broadened. Fig. 3(c)–(e) shows the XRD patterns of the ZrO_2 freeze dried precursor powders calcined at 1173 K for 30 to 120 min, and it can be seen that the ZrO_2 still maintained the single tetragonal phase, but the intensity and peak width did not demonstrate any variations. This phenomenon is due to the fact that when the ZrO_2 freeze dried precursor powders are calcined at 1173 K for various periods of time, the calcination temperature is only slightly greater than the crystallization temperature; therefore, the Zr and O atoms do not obtain enough energy for rearrangement to the lattice position leading to the crystallization. Hence, the poor crystallinity and broadening of the XRD patterns is still maintained when the ZrO_2 freeze-dried precursor powders are calcined at 1173 K for 10 to 120 min.

3.3. Phase stability of t-ZrO_2

Fig. 4 shows the XRD patterns of the ZrO_2 freeze dried precursor powders prepared in a silica bath calcined at 1473 K for various periods of time. It indicates that all of the patterns still maintain the single t-ZrO_2phase; however, the intensity variations in the reflections are very obvious. Fig. 4(b) demonstrates the XRD pattern of the ZrO_2 freeze dried precursor powders calcined at 1473 K for 30 min, and it can be seen that only the single phase of t-ZrO_2 appears. In contrast to Fig. 4(a) (calcination at 1473 K for 10 min), it can also be seen that the intensity of (101)

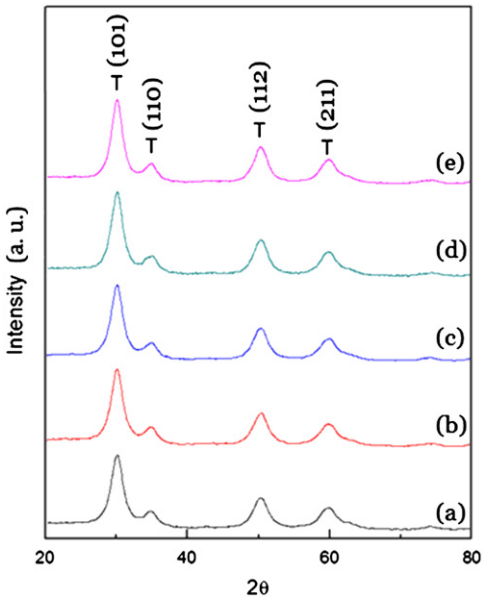

Fig. 3. XRD patterns of the tetragonal zirconia freeze dried precursor powders are calcined at 1173 K for various times: (a) 10 min, (b) 20 min, (c) 30 min, (d) 60 min and (e) 120 min. (T: tetragonal zirconia).

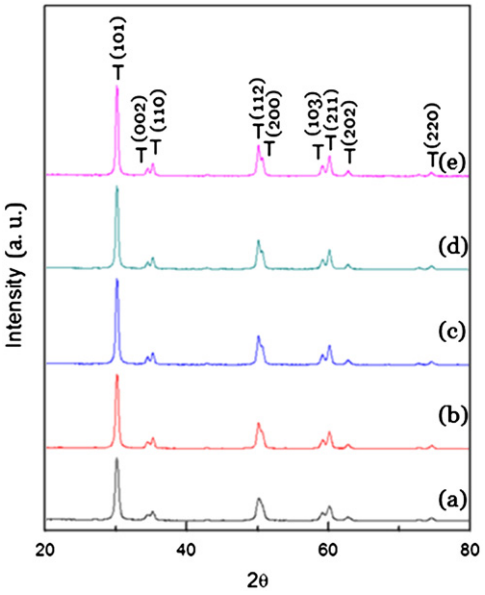

Fig. 4. XRD patterns of the tetragonal zirconia freeze dried precursor powders are calcined at 1473 K for various times: (a) 10 min, (b) 20 min, (c) 30 min, (d) 60 min and (e) 120 min. (T: tetragonal zirconia).

reflection increases, and the full-width at half-maximum intensity (FWHM) decreases. In addition, except the degree to which the (002) and (110), (103) and (211) reflection splits still increase, the (112) and (200) reflections are also slightly split. This is because of the formation of an almost complete t-ZrO_2 crystallite structure.

The XRD patterns of the synthesized ZrO_2 powders are shown in Fig. 4(c)–(e) when the ZrO_2 freeze dried precursor powders calcined at 1473 K for 30 to 120 min. This indicates that all the reflection peaks still maintained the t-ZrO_2 without other phases being detected. On the other hand, it can also be seen that the intensity of the (101) reflection peak increases with calcination time. The FWHM of the (101) reflection slightly decreases with time. This is due to the fact that calcination at 1473 K for 30 to 120 min only provides an adequate aging time for the formation and growth of t-ZrO_2 crystallite. However, there is no obvious change in the intensity and split of (112) and (200) reflections when calcination time is increased to 120 min because the t-ZrO_2 crystallite structure becomes stable when calcined at 1473 K for 120 min.

3.4. The crystallite size of the t-ZrO_2 for freeze-dried precursor powders after calcination

The crystallite sizes of the t-ZrO_2 for freeze dried precursor powders calcined at various temperatures for different time periods are shown in Fig. 5. It can be seen that the crystallite size of t-ZrO_2 was only about 3.0 nm when calcined at 1173 K for 10 to 120 min because the t-ZrO_2 crystallites did not obtain enough energy for crystallite growth when calcined at 1173 K. The crystallite size of t-ZrO_2 slightly increased to 4.0 nm when calcined at 1273 K for 10 to 120 min. This was also caused by the calcination temperature not having provided enough energy for crystallite growth. It can be seen that the t-ZrO_2 crystallite size increased from about 4.0 to 8.5 nm when the calcination temperature rose from 1273 to 1473 K. Moreover, the crystallite size of the t-ZrO_2 rapidly increased from 8.5 to 16.7 nm when calcined at 1473 K for 10 to 30 min. However, the crystallite size of t-ZrO_2 only slightly increased from 16.7 to 19.2 nm with the calcination time was increased from 30 to 120 min. This result is due to the fact that the t-ZrO_2 can obtained enough energy for crystallite growth when calcined at 1473 K for 10 to 30 min. When the calcination time was prolonged from 30 to 60 min, it is possible that on the surface of t-ZrO_2 surrounding by amorphous SiO_2 limiting the t-ZrO_2 crystallite growth. On the other hand, the results shown in Fig. 5 also show that the crystallite size of t-ZrO_2 increased with the calcination temperature when held for a fixed time.

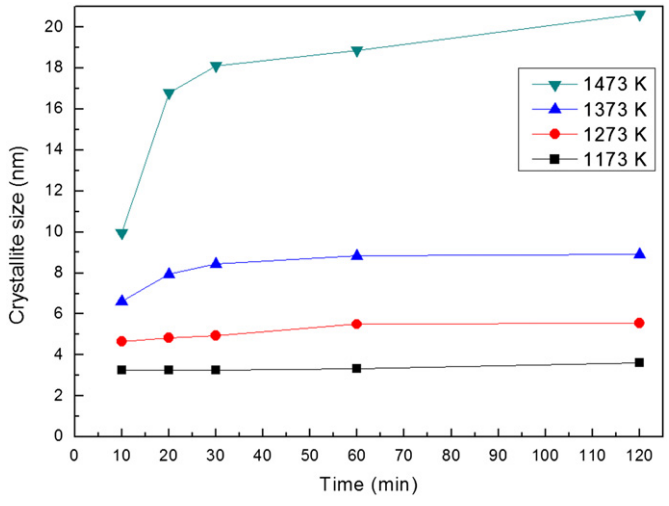

Fig. 5. Crystallite size of the tetragonal zirconia for the freeze dried precursor powders prepared in silica bath are calcined at various temperatures and times.

3.5. The TEM microstructure of the ZrO_2 freeze-dried precursor powders after calcination

The TEM micrographs and EDS analyses of the tetragonal zirconia freeze-dried precursor powders calcined at 1173 K for 1 h are shown in Fig. 6. Fig. 6(a) and (b) show the bright field (BF) and dark field (DF) images of the crystallites with a size of about 2 to 4 nm, which is consistent with the results shown in Fig. 5. Fig. 6(c) shows the SAED pattern, the index for which corresponds with the tetragonal zirconia. This result also provides evidence for the presence a single phase of t-ZrO_2 in the calcination sample. Fig. 6(d) shows an image of high resolution TEM, which indicates that the d-spacings of (101), (110), and (002) of the t-ZrO_2 are 2.95 Å, 2.54 Å, and 2.57 Å, respectively. Site "f" denotes an amorphous area, indicating that the t-ZrO_2 was surrounded by the amorphous silica. The EDS analyses are shown in Fig. 6(e), and it can be seen that the sample contain the atoms of the O, Si and Zr. Although the atomic ratio of Zr, and Si is approximately to 1:1, the SiO_2crystallites are not shown in Figs. 2–4. According to the results shown in Fig. 6(e), the surrounding substance on the t-ZrO_2 surface is amorphous SiO_2 (a-SiO_2).

Fig. 7 shows the micrographs and EDS analyses of the zirconia freeze-dried precursor powders calcined at 1473 K for 1 h. Fig. 7(a) and (b) show the (BF) and (DF) images, and crystallites with a size of about 15 to 20 nm can be seen. This result is also consistent with the results shown in Fig. 6. Fig. 7(c) shows the SAED pattern, the index for which corresponds with the tetragonal zirconia. This result indicates that the tetragonal zirconia freeze-dried precursor powders calcined at 1473 K for 1 h still maintained the single tetragonal phase. Fig. 7(d) shows a high resolution TEM image. It can be seen that the crystallite size of the t-ZrO_2 is about 22 nm, with d-spacings of (101) was 2.95 Å. In addition, the interface between the two crystallites of t-ZrO_2 contained an amorphous substance. Fig. 7(e) shows the EDS analyses of Fig. 7(a), and it can be seen that the sample contained O, Si and Zr atoms but that only t-ZrO_2 appears in the XRD pattern. According to the results shown in Fig. 7(d), it can be seen that SiO_2 is still absorbed on the t-ZrO_2 surface and maintains an amorphous state [30].

Fig. 8 shows the micrographs and EDS analyses of the zirconia freeze-dried precursor powders are calcined at

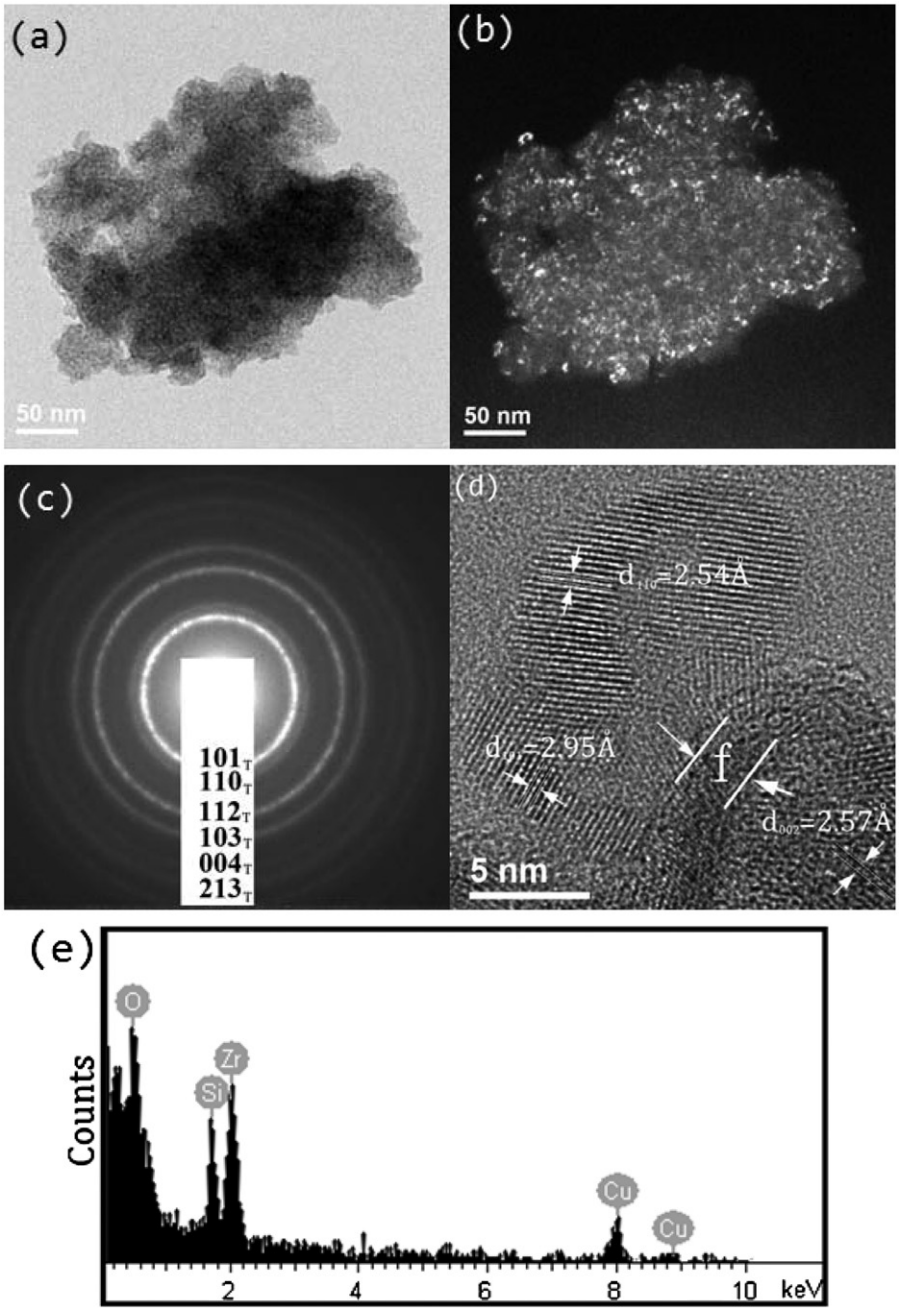

Fig. 6. TEM micrographs of the tetragonal zirconia freeze dried precursor powders are calcined at 1173 K for 1 h: (a) BF image, (b) DF image, (c) SAED pattern and (d) high resolution lattice image, and (e) EDS analyses.

1473 K for 1 h. Fig. 8(a) shows the bright field (BF) image, Fig. 8(b) shows the dark field (DF) image of the (101) of tetragonal crystallites denoted by $(101)_t$, it is seen that the crystallites with the size of about 15 to 24 nm. This result also consistent with the results of Fig. 6. Fig. 8(c) shows the SAED pattern, which index corresponds to the tetragonal zirconia. This result indicates that when the zirconia freeze-dried precursor powders calcined at 1473K for 1 h are still maintain the single tetragonal phase. Fig. 8(d) shows an image of high resolution TEM. It is seen that the crystallite size of the t-ZrO_2 is about 20 nm. In addition, the interface between the two crystallites of t-ZrO_2 have a area of amorphous substance exist. Fig. 8(e) shows the SAED pattern in the region marked "1" in Fig. 8(d), the result also indicates that the crystallite of zirconia freeze-dried precursor powders are calcined at 1473 K for 1 h still maintain the tetragonal phase and the indexed SAED pattern shows (112), and planes along the $[0\bar{2}1]$ zone axis. Fig. 8(f) shows the EDS analyses of the Fig. 8(d) in the region marked "1", it is seen that the sample contain the atoms of O, Si and Zr, but only t-ZrO_2 appear in the XRD pattern. Fig. 8(g) shows the SAED pattern in the region marked "2" in Fig. 8(d), the result indicates that the substance which surrounded the crystallite were

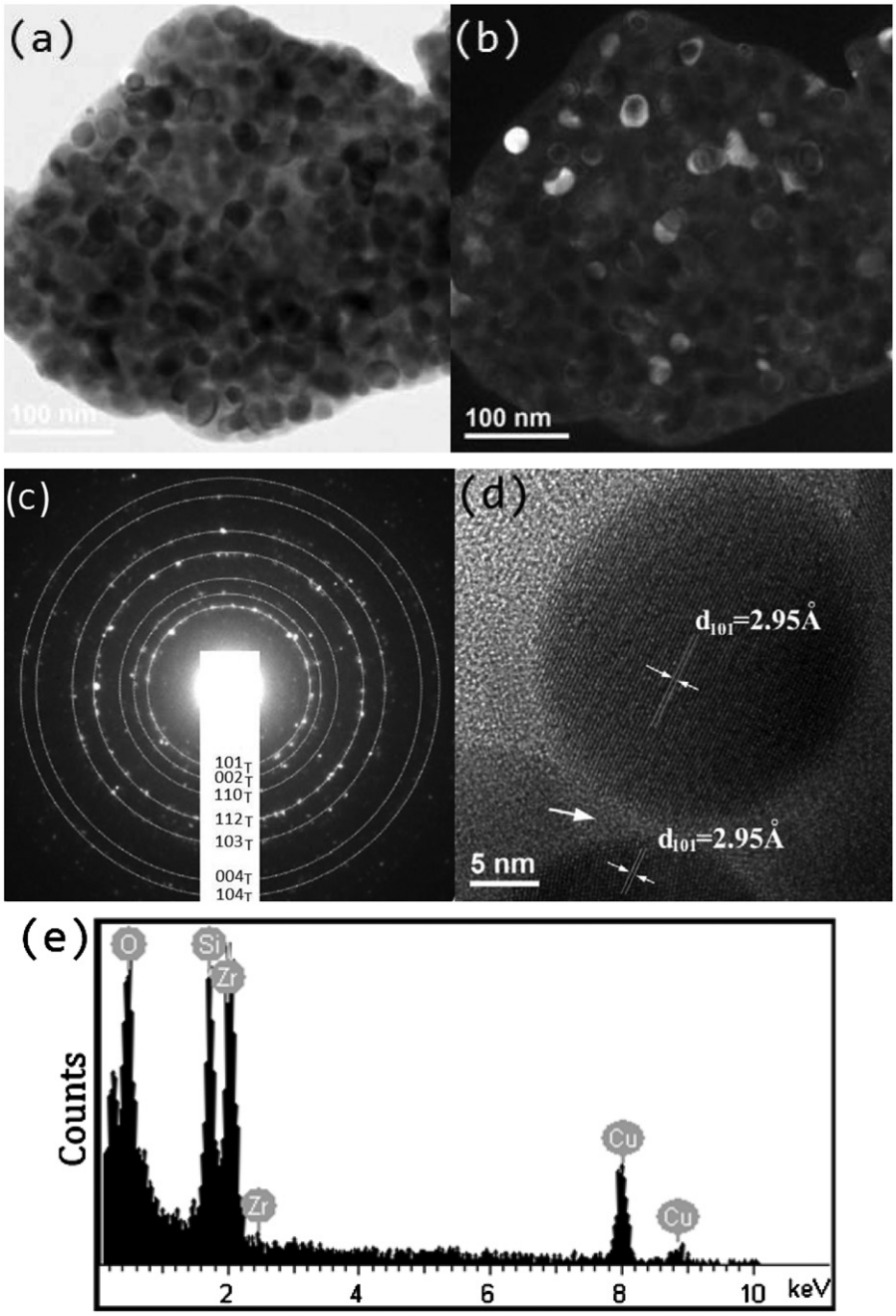

Fig. 7. TEM micrographs of the tetragonal zirconia freeze dried precursor powders are calcined at 1473 K for 1 h: (a) BF image, (b) DF image, (c) SAED pattern, (d) high resolution lattice image, and (e) EDS analyses.

amorphous. Fig. 8(h) shows the EDS analyses of the Fig. 8(d) in the region marked "2", the atomic ratio of the sample contained was O: Si: Zr = 51.06: 26.77: 22.17, the high proportional contain of Si, shows the confirmation of the tetragonal zirconia crystallite was surrounded by the amorphous silica.

According to Figs. 6–8, the energy peak lower than the O atomic perhaps most due to the carbon from the coating of copper grid and other atomic numbers smaller than oxygen. Cu atom was due to the copper grid used in TEM analysis.

4. Discussion

4.1. Thermal behavior of ZrO_2 freeze-dried precursor powders

In the previous study of Hsu et al. [13], zirconium (IV) nitrate ($Zr(NO_3)_4 \cdot xH_2O$) and yttrium nitrate hexahydrate ($Y(NO_3)_3 \cdot 6H_2O$) were used as the starting materials, and they pointed out that when the temperature was higher than 1020 K, the weight loss of ZrO_2 freeze-dried precursor powders in the TG analysis no longer occurred.

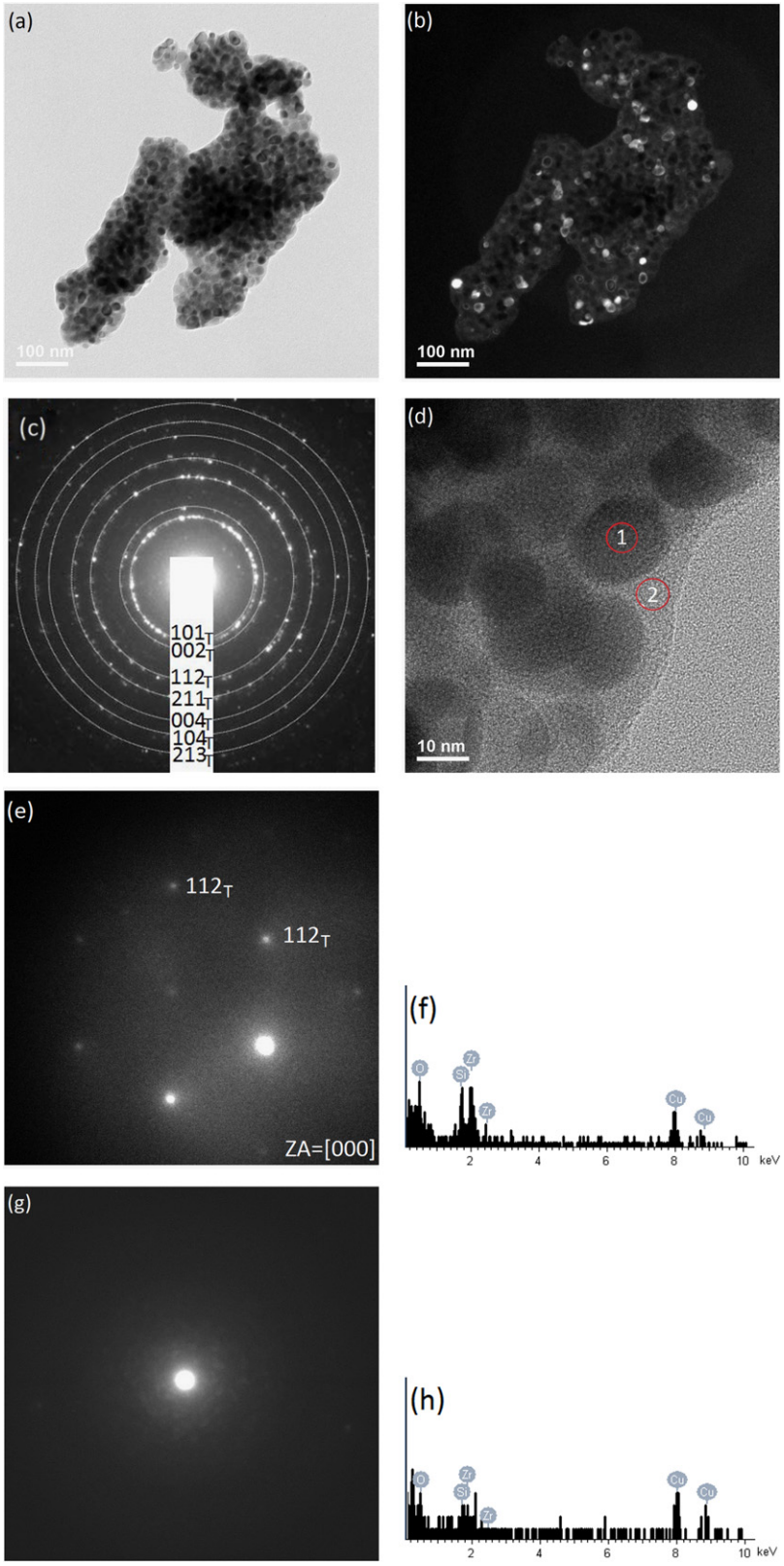

Fig. 8. TEM micrographs of the tetragonal zirconia freeze dried precursor powders are calcined at 1473 K for 1 h: (a) BF image, (b) (101)t DF image, (c) SAED pattern, (d) high resolution lattice image, (e) SAED pattern of the Fig. 8(d) in the region marked "1", (f) EDS analysis of the Fig. 8(d) in the region marked "1", (g) SAED pattern of the Fig. 8(d) in the region marked "2" and (f) EDS analysis of the Fig. 8(d) in the region marked "2".

This result corresponded to those in the present study. Moreover, Whitney [29] also pointed out that the ZrO_2 in the $ZrO_2 \cdot 6H_2O$, which corresponds to a residual of 53 wt%, was due to the base and zirconyl ion metathetical reaction. In the present study, corresponding to $ZrO_2 \cdot 2H_2O$, the freeze-dried precursor powders contained about 75.7 wt% ZrO_2.

4.2. The phase transformation of the ZrO_2 freeze-dried precursor powders after calcination

Furthermore, from Fig. 2 it can also be seen that with the exception of the reflections of a single phase t-ZrO_2, no other phases can be detected when the ZrO_2 freeze dried precursor powders are calcined from 1173 K to 1473 K for 10 min. This result is in agreement with the report of Hsu et al. [13].

The freeze dried precursor powders of 3 mol% yttria-partially stabilized zirconia were obtained using $ZrOCl_2$ and $Y(NO_3)_3$ as raw materials via a coprecipitation method in an alcohol-water solution following the research of Kuo et al. [28]. They pointed out the highest exothermic peak at 700 K to be due to the tetragonal to monoclinic ZrO_2 transition. When the 3Y–PSZ freeze dried precursor powders are calcined at 703 to 1073 K for 2 h, the crystal structure is composed of tetragonal and monoclinic ZrO_2. The results of Kuo et al. [28] are not in agreement with the present study. This phenomenon may be a result of the use of different starting materials. On the other hand, Veytizou et al. [30] used TEOS and $ZrO(NO_3)_2 \cdot 6H_2O$ as the starting materials for preparation of zircon precursor powders using sol–gel processing. They pointed out that an exothermic peak was observed at about 1173 K in the DTA curve and attributed this to the phase transformation from amorphous ZrO_2 into the t-ZrO_2. This result is in agreement with the present study. In addition, Veytizou et al. [30] also purposed the presence of crystalline zircon when the precursor powders dried at 373 K. Furthermore, they also pointed out that their XRD results showed that total transition to zircon becomes possible at temperatures higher than 1273 K as a result of the reaction between t-ZrO_2 and unreacted amorphous silica (a-SiO_2) [30]. This result is also not in agreement with the present study.

4.3. Phase stability of t-ZrO_2

Veytizou et al. [30,31] pointed out that the XRD pattern of the precursor powders obtained for the $ZrO(NO_3)_2 \cdot 6H_2O$ and TEOS mixed in a 100°C water for 24 h shows that a lot of zircon is already partially crystallized. When the bodies of these precursor powders are sintered at 1473 K for 3 h, the phase compositions of the zircon and t-ZrO_2 appear as the major and minor phases, respectively. Furthermore, when sintering at 1473 K for 6 h, it only contains a single zircon phase [31]. These results do not correspond to those of the present study, which may be a result of the different starting materials and processes.

Kirsch et al. [32] used zirconium chloride and aluminum isopropoxide as the starting materials to synthesize amorphous precursor powders coated with alumina. When calcined below 1073 K for 2 h, the XRD patterns were amorphous, and when calcined at 1323 K and 1373 K for 2 h, the XRD patterns showed the tetragonal single phase. Furthermore, when calcined at 1473 K for 2 h, the phases were composed of the t-ZrO_2 and α-almina as the major and minor phases, respectively. These results were similar to those of the present study, but in the present study, the coating material could not be seen in the XRD pattern.

In addition, the well-known inversion in silica at 846, 1140 and 1473 K are included in the ZrO_2–SiO_2 phase diagram [33], retention of the 1140 and 1473 K inversion the zircon and tridymite for the SiO_2 greater than 30 wt%. In the present study, the mole ratio of ZrO_2: SiO_2 is 1:1, but the zircon and tridymite are not shown in the XRD pattern when the ZrO_2 freeze dried precursor powders are calcined at 1473 K for 120 min, which is not agreement with the ZrO_2–SiO_2 phase diagram [33]. This result may be due to the different starting materials and the length and temperature of calcination (1473 K for 120 min).

4.4. The crystallite size of the t-ZrO_2 for freeze-dried precursor powders after calcination

According to the results shown in Figs. 2–5, it can be seen that the t-ZrO_2 demonstrated excellent phase stability when the ZrO_2 freeze dried precursor powder was calcined at 1173 to 1473 K for 120 min. This phenomenon can be attributed to the fact that the size of the all of the crystallites did not exceed the critical value of 30 nm, for the t-ZrO_2 transition to m-ZrO_2 [5]; therefore, in order for the entire sample to be t-ZrO_2, this structure must have a lower surface energy than the m-ZrO_2 phase [34].

Assuming that the new homogeneous phase as formed, that they have an equilibrium composition with sharply defined phase boundaries with no stresses, and that the value of the interfacial energy does not depend on the curvature of the boundary, the change in the free energy accompanying the formation can be expressed as the sum of one proportional to the volume and the second to the surface area. Let the new regions be spherical in shape with a radius r; then the change of the free energy (ΔG) of two polymorphs can be given by [34]

$$\Delta G_r = \frac{4}{3}\pi r^3(\psi' - \psi) + 4\pi r^2(\sigma' - \sigma). \quad (5)$$

where r is the radius of a crystallite; ψ is the free energy of the unit volume of a radius of spherical crystallite; σ is the surface free energy of the crystallite, and primed symbols refer to the high temperature phase.

The critical size of radius, r_c, can be found from the condition of $\partial \Delta G_r / \partial r = 0$

$$r_c = -2\frac{\sigma' - \sigma}{\psi' - \psi}. \quad (6)$$

Garvle [34] expanded the term of $(\Psi' - \Psi)$ using a Taylor's series about the transformation temperature of an infinite crystallite, and expressed Eq. (6) in a useful form:

$$r_c = -2\frac{\sigma' - \sigma}{Q(1-(T/T_b))}. \quad (7)$$

where Q is the heat of transformation of unit volume of an infinite crystallite, and T_b is the transformation temperature of an infinite crystallite.

Holmes et al. [35] studied the immersion heat of a ZrO_2–H_2O system and used Eq. (7) to obtain strong evidence that the surface free energy of m-ZrO_2 is greater than that of t-ZrO_2. They pointed out that in the range 873–1073 K, the ZrO_2 powders were tetragonal, and the crystallite size increased from 8 to 13 nm. When the samples were calcined in the range 1073 K and 1173 K, the crystallites grew to 22 nm and contained a trace amount of m-ZrO_2 due to having some crystallite sizes that were greater than a critical size. When at 1273 K, the crystallites grew to 26 nm, converting the entire sample to m-ZrO_2 because the size of all of the crystallites exceeded the critical value. The results of present study are not in agreement with the Holmes et al. [35] except at 1073 K due to the crystallite size smaller than that of 20 nm when calcination at 1473 K for 120 min. This value did not exceed the critical value, so the entire sample was t-ZrO_2.

In addition, for any phase transformation of a solid state associated with an endothermic heat effect when heating, there must be critical crystallite sizes below which the high temperature structure is stable at temperatures much lower than the bulk transformation temperature also proposed by Garvie [36] and Filipovich and Kalinina [37]. In the present study, the crystallite size was below than that of 20 nm when calcined at 1473 K for 120 min. This value is much lower than that of 30 nm [5], which is because the surface of the t-ZrO_2 absorbs the amorphous SiO_2 (a-SiO_2) and thus inhibits the crystallite growth of t-ZrO_2. Therefore, the ZrO_2 crystallites have excellent tetragonal stability when the ZrO_2 freeze dried precursor powders are calcined at 1473 K for 120 min.

5. Conclusions

The phase formation and stability of the tetragonal ZrO_2 prepared in a silica bath was investigated using DSC/TG, XRD, TEM, SAED and EDS. These results of this study are summarized as follows:

(1) From the results of the thermal analyses, it was determined that the main compound of the ZrO_2 freeze dried precursor powders was $ZrO_2 \cdot 2H_2O$ and that the t-ZrO_2 was formed at 1165 K.
(2) The results of the XRD showed the single phase of t-ZrO_2 when the ZrO_2 freeze-dried precursor powders were calcined at 1173–1473 K for 2 h.
(3) The crystallite size of t-ZrO_2 increased from 3 to 19 nm when the ZrO_2 freeze dried precursor powders were calcined at 1173 K to 1473 K for 120 min.
(4) The tetragonal phase of ZrO_2 had excellent stability when the ZrO_2 freeze dried precursor powders were calcined at 1473 K for 120 min due to the absorption of amorphous SiO_2 (a-SiO_2) on the t-ZrO_2 surface, inhibiting the crystallite growth of t-ZrO_2.
(5) The results from the high resolution lattice image and the IFFT image showed that the tetragonal zirconia was surrounded by the amorphous silica.

Acknowledgments

The authors sincerely thank the National Science Council of Taiwan for its financial support under NSC 100-2622-E-037-001-CC3. We also wish to thank Professor I. M. Hung for DSC/TG and Mr. H. Y. Yao for TEM and EDS.

References

[1] Y.M. Chiang, D. Birnie III, W.D. Kingery, Physical Ceramics: Principles for ceramic science and engineering, Wiley, 1997.
[2] H. Heuer, Transformation toughening in ZrO_2-containing ceramics, Journal of the American Ceramic Society 70 (1987) 689–698.
[3] X.Q. Cao, R. Vassen, D. Stoever, Ceramic materials for thermal barrier coatings, Journal of the European Ceramic Society 24 (2004) 1–10.
[4] R.H.J. Hannink, P.M. Kelly, B.C. Muddle, Transformation toughening in Zirconia-containing ceramics, Journal of the American Ceramic Society 83 (2000) 461–487.
[5] R.C. Garvie, R.H. Hannink, R.T. Pascoe, Ceramic steel?, Nature 258 (1975) 703–704
[6] A.H. Heuer, L.W. Hobbs (Eds.), Science and Technology of Zirconia, Vol. 3, American Ceramic Society, Columbus, OH, 1981.
[7] N. Claussen, M. Rühle, A.H. Heuer (Eds.), Science and Technology of Zirconia II, Vol. 12, American Ceramic Society, Columbus, OH, 1985.
[8] S.P.S. Badwal, M.J. Bannister, R.H.J. Hannink (Eds.), Science and Technology of Zirconia V. Technomic, Lancaster, PA, 1993.
[9] A.G. Evans, Perspective on the development of high-toughness ceramics, Journal of the American Ceramic Society 73 (1990) 187–206.
[10] C. Pascual, P. Duran, Subsolidus phase equilibria and ordering in the system ZrO_2–Y_2O_3, Journal of the American Ceramic Society 66 (1983) 23–27.
[11] J.L. Shi, B.S. Li, Z.L. Lu, X.X. Huang, Correlation between microstructure, phase transformation during fracture and the mechanical properties of Y-TZP ceramics, Journal of the European Ceramic Society 16 (1996) 795–798.
[12] C.W. Kuo, Y.H. Lee, I.M. Hung, M.C. Wang, S.B. Wen, K.Z. Fung, C.J. Shih, Crystallization kinetics and growth mechanism of 8 mol% yttria-stabilized zirconia (8YSZ) nano-powders prepared by a sol–gel process, Journal of Alloys and Compounds 453 (2008) 470–475.
[13] Y.W. Hsu, K.H. Yang, K.M. Chang, S.W. Yeh, M.C. Wang, Synthesis and crystallization behavior of 3 mol% yttria stabilized tetragonal zirconia polycrystals (3Y-TZP) nanosized powders prepared using a simple co-precipitation process, Journal of Alloys and Compounds 509 (2011) 6864–6870.
[14] E.N.S. Muccillo, E.C.C. Souza, R. Muccillo, Synthesis of reactive neodymia-doped zirconia powders by the sol–gel technique, Journal of Alloys and Compounds 344 (2002) 175–178.
[15] J.K. Lee, H.H. Kang, Ceria-stabilized zirconia ceramics with irregular grain shapes, Materials Letters 42 (2000) 215–220.
[16] J.C. Ray, A.B. Panda, P. Pramanik, Chemical synthesis of nanocrystals of tantalum ion-doped tetragonal zirconia, Materials Letters 53 (2002) 145–150.

[17] C. Valent n, J.V. Folgado, J. Alarcón, Low-temperature metastabilization of tetragonal V^{+4}-containing ZrO_2 solid solutions, Materials Research Bulletin 36 (2001) 1615–1627.
[18] A.C. Bose, R. Ramamoorthy, S. Ramasamy, Formability of metastable tetragonal solid solution in nanocrystalline NiO–ZrO powders, Materials Letters 44 (2000) 203–207.
[19] C. Radloff, N.J. Halas, Enhanced thermal stability of silica-encapsulated metal nanoshells, Applied Physics Letters 79 (2001) 674–676.
[20] S. Ramesh, E. Sominska, A. Gedanken, Synthesis and characterization of submicrospherical silica particles uniformly coated with nanocrystalline yttria stabilized zirconia, Ultrasonics Sonochemistry 9 (2002) 61–64.
[21] R. Ramamoorthy, R. Chaim, Microstructural evolution in nanocrystalline Y–TZP containing a silicate glass, Journal of the European Ceramic Society 21 (2001) 2895–2902.
[22] R. Ramamoorthy, R. Chaim, Sintering and microstructure of glass-coated nanocrystalline yttria-stabilized tetragonal zirconia powder: effect of the glass, Journal of Materials Research 16 (2001) 296–302.
[23] S.H. Tolbert, A.B. Herbold, L.E. Brus, A.P. Alivisatos, Pressure-induced structural transformations in Si nanocrystals: surface and shape effects, Physical Review Letters 76 (1996) 4384–4387.
[24] B.D. Cullity, Elements of X-ray Diffraction, Addison-Wesley, Reading, MA, 1967, p. 170.
[25] G.K. Chuah, S. Jaenicke, B.K. Pong, The preparation of high-surface-area zirconia. II. Influence of precipitating agent and digestion on the morphology and microstructure of hydrous zirconia, Journal of Catalysis 175 (1998) 80–92.
[26] C.L. Kuo, C.L. Wang, H.H. Ko, W.S. Hwang, K.M. Chang, W.L. Li, H.H. Huang, Y.H. Chang, M.C. Wang, Synthesis of zinc oxide nanocrystalline powders for cosmetic applications, Ceramics International 36 (2010) 693–698.
[27] H.S. Liu, T.S. Chin, S.Y. Chiu, K.H. Chung, C.S. Chang, M.T. Liu, Hydroxyapatite synthesized by a simplified hydrothermal method, Ceramics International 23 (1997) 19–25.
[28] C.W. Kuo, Y.H. Shen, S.B. Wen, H.E. Lee, I.M. Hung, H.H. Huang, M.C. Wang, Phase transformation kinetics of 3 mol% yttria partially stabilized zirconia (3Y-PSZ) nanopowders prepared by a non-isothermal process, Ceramics International 37 (2011) 341–347.
[29] E.D. Whitney, Observations on the nature of hydrous zirconia, Journal of the American Ceramic Society 53 (1970) 697–698.
[30] C. Veytizou, J.F. Quinson, O. Valfort, G. Thomass, Zircon formation from amorphous silica and tetragonal zirconia: kinetic study and modeling, Solid State Ionics 139 (2001) 315–323.
[31] C. Veytizou, J.F. Quinson, Y. Jorand, Preparation of zircon bodies from amorphous precursor powder synthesized by sol–gel processing, Journal of the European Ceramic Society 22 (2002) 2901–2909.
[32] B.L. Kirsch, S.H. Tolbert, Stabilization of isolated hydrous amorphous and tetragonal zirconia nanoparticles through the formation of a passivating alumina shell, Advanced Functional Materials 13 (2003) 281–288.
[33] W.C. Butterman, W.R. Foster, Zircon stability and the ZrO_2–SiO_2 phase diagram, American Mineralogist 52 (1967) 880–885.
[34] R.C. Garvie, Stabilization of the tetragonal structure in zirconia microcrystals, The Journal of Physical Chemistry 82 (1978) 218–224.
[35] H.F. Holmes, E.L. Fuller Jr., R.B. Gammage, Heats of immersion in the zirconium oxid-water system, The Journal of Physical Chemistry 76 (1972) 1497–1502.
[36] R.C. Garvie, The occurrence of metastable tetragonal zirconia as a crystallite size effect, The Journal of Physical Chemistry 69 (1965) 1238–1243.
[37] V. Filipovich, A. Kalinina, Structural transformations in glasses at high temperatures, Structure of Glass, 5, (1965) 34.